

# Application of Dielectric, Ferroelectric and Piezoelectric Thin Film Devices in Mobile Communication and Medical Systems

M. Klee<sup>1</sup>, D. Beelen<sup>1</sup>, W. Keur<sup>1</sup>, R. Kiewitt<sup>2</sup>, B. Kumar<sup>1</sup>, R. Mauczok<sup>1</sup>,  
 K. Reimann<sup>1</sup>, Ch. Renders<sup>1</sup>, A. Roest<sup>1</sup>, F. Roozeboom<sup>1</sup>, P. Steeneken<sup>1</sup>, M. Tiggelman<sup>1</sup>,  
 F. Vanhelmont<sup>1</sup>, O. Wunnicke<sup>1</sup>, P. Lok<sup>3</sup>, K. Neumann<sup>3</sup>, J. Fraser<sup>4</sup> and G. Schmitz<sup>5</sup>

<sup>1</sup> Philips Research, High-Tech Campus 4, , 5656 AE Eindhoven, The Netherlands,  
 Fax.: 0031402746505, mareike.klee@philips.com

<sup>2</sup> Philips Research Aachen, <sup>3</sup> Philips Semiconductors, <sup>4</sup> Philips Medical Systems Ultrasound, <sup>5</sup> University of Bochum,

**ABSTRACT :** Dielectric, ferroelectric and piezoelectric thin films are getting more and more attention for next generation mobile communication and medical systems. Thin film technologies based on dielectric, ferroelectric and piezoelectric thin films enable System-in-Package (SiP) devices, resulting in optimal integration of various functions in one module with respect to high performance, small size and low cost. Within Philips a passive integration platform for SiP technologies is developed, comprising key functions such as RF filters, micro-electromechanical switches, high-value capacitors as well as passive and active functions integrated in small modules. The piezoelectric thin film technologies do not only play a role for RF filters, but are also a breakthrough technology for a new class of thin film ultrasonic transducers.

**Keywords :** dielectric, ferroelectric, piezoelectric thin films, System in Package, thin film ultrasonic transducers

## 1. INTRODUCTION

System integration is moving ahead with higher functionality, improved performance, further miniaturization and cost-effective implementations. World wide two system integration paths are followed. System-on-chip is focusing on integration of all functions on one die. Here the technology for baseline CMOS follows the smallest dimensions as predicted by Moore's law (see Fig. 1)

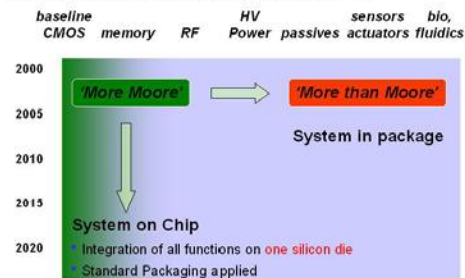


Figure 1: Integration trends.

A complementary technology is **System-in-Package (SiP)**, which aims at integrating various functions in one module. Here, individual functions are implemented in their optimum technology with respect to high performance, small size, low cost. Main reasons to offer SiP devices are multi-functional modules, which enable different die technologies in one package and thus enhanced functionality and fast time-to-market. SiP plays an important role for the integration of functions, which request non-traditional materials and processes, which are not available in standard CMOS technologies. These can comprise for example functions such as capacitors, resistors, inductors, filters, non-semiconductor switches. These require non-traditional materials such as dielectric, ferroelectric, or piezoelectric thin films, which are not available in standard CMOS tech-

nologies. System in package technologies are here the optimum approach to achieve small size, high performance and a fast time to market. System in Package technologies are intensively investigated for next generation mobile communication systems, where there is the trend from single/dual mode systems with multiple chipsets to multi-band, multi-mode systems with multimedia capabilities (see Fig. 2). To achieve a small form factor in multi-band, multi-mode devices, a higher level of integration has to be achieved. Furthermore, concepts have to be developed, which enable re-configurable circuits that support more than one frequency band in a versatile device.

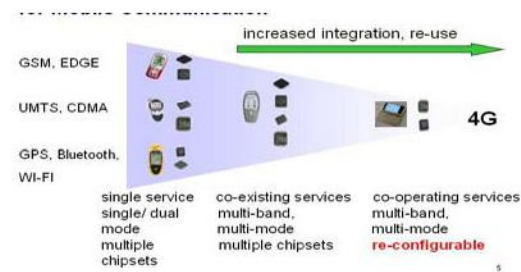


Figure 2: Trends in mobile communication systems.

On the way to miniaturisation and improved performance of System in Package devices, dielectric, ferroelectric, and piezoelectric thin films play an important role. Some applications will be discussed in the following.

## 2. DIELECTRIC, FERROELECTRIC AND PIEZOELECTRIC THIN FILMS IN SYSTEM IN PACKAGE

### 2.1. Bulk acoustic wave filter

One of the key functions in RF front-end modules is high-frequency filtering. The miniaturization trend has led to the development of electro-acoustic devices since the acoustic wavelength is 5 orders of magnitude smaller than the electromagnetic wavelength. Presently surface acoustic wave (SAW) filters are used. In these filters surface acoustic waves are excited by interdigital electrodes deposited on the surface of a piezoelectric single crystalline material (often  $\text{LiNbO}_3$ ). However, these filters suffer from material problems caused by acoustomigration at the high power levels of 1–3 W that are used in mobile phones. This leads eventually to shorts in the interdigital electrodes, which are spaced less than 1  $\mu\text{m}$  apart. Furthermore a relatively high temperature drift of frequency is observed in these devices. Bulk acoustic wave (BAW) filters, in which the thickness extensional mode of a thin piezoelectric film is excited, are more robust. The centre frequency of the filter is determined by the thickness of the layers (typically between a few 100 nm to a few  $\mu\text{m}$  thick). The low temperature drift of about 20 ppm/K is a further advantage. All processes and materials are semiconductor compatible [1].

The piezoelectric layer, most often a highly c-axis oriented AlN film, is sandwiched between the two electrodes which are composed of a high conductivity material like Al, Mo, W, Pt or Ru, see Fig. 3. In order to reduce losses in the BAW filter, the acoustic energy needs to be confined in the resonator. This is realised by an acoustic reflector. The thin film BAW resonator (FBAR) is realised on top of a thin membrane that reflects almost all the acoustic waves at all frequencies [2]. The membrane is realised via micro electro mechanical system (MEMS) techniques. Alternatively, the membrane can be replaced by a Bragg mirror. This consists of alternating layers of high and low acoustic impedance materials like  $\text{SiO}_2/\text{AlN}$ ,  $\text{SiO}_2/\text{W}$  or  $\text{SiO}_2/\text{metal-oxides}$  [3–7]. These resonators are referred to as solidly mounted BAW resonators (SBAR). New piezoelectric materials are under investigation. These might open the possibility of obtaining tuneable filters in the future [8,9,21,36,37].

BAW resonators have two characteristic frequencies: at resonance the electrical impedance  $|Z|$  is very small (polarization and applied electrical field are parallel); at anti-resonance  $|Z|$  is very large (electrical field is anti-parallel to the polarization). A BAW ladder filter consists of two types of resonators: series and shunt resonators. The shunt resonators are slightly shifted to lower frequency by means of mass-loading. In this way the anti-resonance of the shunt resonator coincides with the resonance of the series resonator. In this way a filter is realised with a low insertion loss in the pass-band and strong suppression at other frequencies, see Fig. 4.

BAW resonators can be simulated accurately using a 1-dimensional electro-acoustic model [10]. This predicts most features of the resonator response. It is used to extract important layer parameters like velocity of sound and elastic constants. However, many acoustic loss mechanisms are 2D in nature. Recently we showed that this can be modelled as well [11].

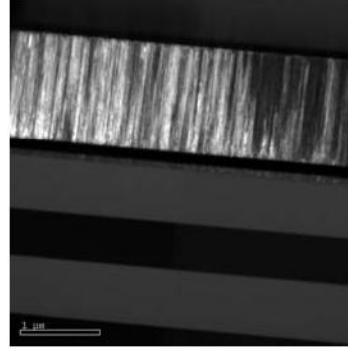


Figure 3: TEM cross section (dark field) through a BAW resonator showing the top layers of the Bragg reflector, the piezoelectric AlN film and the electrodes.

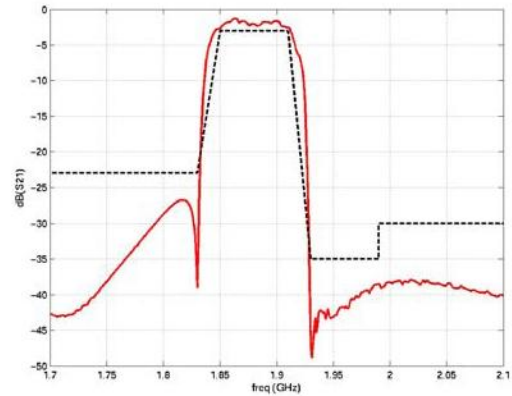


Figure 4: Filter characteristic of a USPCS Tx interstage filter. The dotted line indicates the specifications for the filter.

## 2.2. Piezoelectric switches

Micro-electromechanical (MEMS) switches and tuneable capacitors represent another class of key devices in RF circuits for mobile communication systems. They will allow the realization of re-configurable RF circuits with a frequency agility and power efficiency that is unattainable with conventional semiconducting switching and tuning technologies. Using MEMS, a single transceiver can be readily reconfigured to support different frequency bands [12]. In this way, RF circuitry is re-used, which will lead to a smaller form factor of the transceiver module. Capacitive MEMS switches are developed by several groups based on an electrostatic concept see ref. [13,14]. Another promising technology is based on piezoelectric thin film actuators [15]. Thin film piezoelectric actuators offer large deflections at very low voltages and are therefore attractive for low voltage switches and tuneable capacitors. In figure 5, suspended piezoelectric thin film beam actuators, processed above metal contacts, in semiconductor compatible processes are shown. The piezoelectric actuators show linear dependence of the deflection as a function of voltage with deflections of 1  $\mu\text{m}/\text{V}$  (Fig. 6).

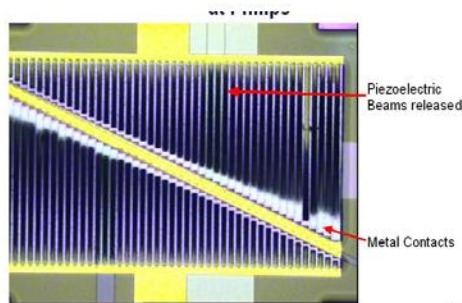


Figure 5a: Piezoelectric thin film actuator processed on Si substrate with metal contact (optical microscopy).

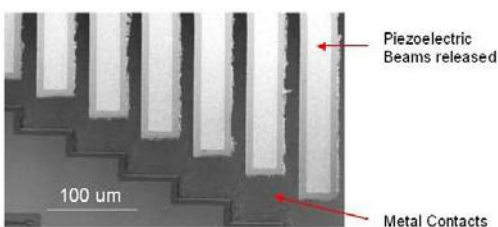


Figure 5b: Piezoelectric thin film actuator processed on Si substrate with metal contact (SEM).

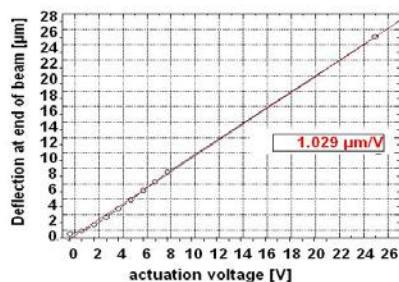


Figure 6: Deflection of thin film piezoelectric actuators as a function of voltage (beam length 320 μm).

### 2.3. Tunable capacitors based on $Ba_{1-x}Sr_xTiO_3$ thin films

In the last few years solid state tunable capacitors were getting more and more attention for tunable RF components. Here the non-linear behaviour of thin film oxides that are based usually on  $Ba_{1-x}Sr_xTiO_3$  films with  $x$  typically 0.25-0.4 is used to realise continuous tunable capacitors. Special features of these tunable capacitors are continuous tuning, high capacitance density and therefore small size, potential of power handling. These capacitors can be used in standard semiconductor integration technologies and do not need any hermetic package. A good reliability is expected for these thin film devices, since they do not contain mechanical parts.  $Ba_{1-x}Sr_xTiO_3$  thin films but also other material systems such as  $Ba_{0.96}Ca_{0.04}Ti_{0.84}Zr_{0.16}O_3$  or  $Bi_{1.5}Zn_{1.0}Nb_{1.5}O_7$  are processed on substrates such as sapphire, polished aluminium oxide ceramics, MgO or high-ohmic Si [16–21,40,41]. In the centre of the investigations

are devices such as tuneable filters, tuneable capacitors for adaptive impedance matching, tuneable phase shifters and voltage controlled oscillators [22–24].

Figure 6 shows a typical tuning curve for a  $Ba_{0.7}Sr_{0.3}TiO_3$  thin film capacitor with a tuneability of 1:4. The capacitors show low current densities of  $1 \cdot 10^{-10}$  A/cm<sup>2</sup> at 30-100 kV/cm (see Fig. 7) and breakdown fields of 0.7-0.9 MV/cm. The  $Ba_{0.7}Sr_{0.3}TiO_3$  thin film capacitors exhibit very little dispersion of the capacitance (see Fig. 8).

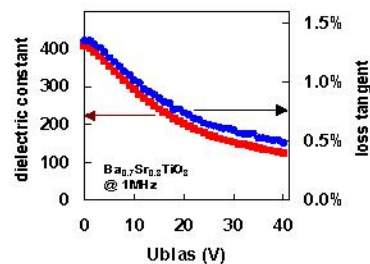


Figure 6: Relative permittivity and loss tangent as a function of dc bias voltage for a  $Ba_{0.7}Sr_{0.3}TiO_3$  thin film.

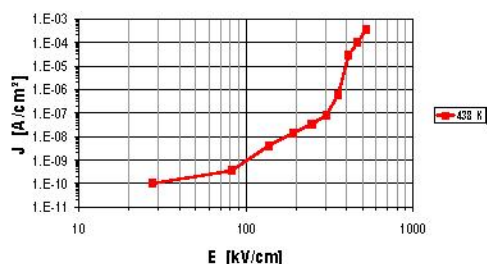


Figure 7: Current density as a function of electric field for a  $Ba_{0.7}Sr_{0.3}TiO_3$  thin film. Measurements carried out at 438 K, data taken after 1000 s.

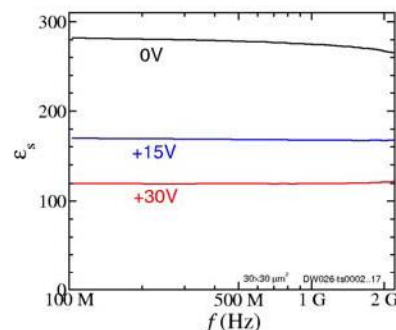


Figure 8: Dielectric constant for 0, 15 and 30 V for a  $Ba_{0.7}Sr_{0.3}TiO_3$  thin film capacitor as a function of frequency.

### 2.4. Integrated capacitors in System in Package

Integration of passive functions (capacitors, resistors and inductors) with active functions into miniaturized modules is a prerequisite for next generation RF front-end as well as next generation base-band, audio and power circuits for

mobile and portable electronic systems. Integration into Systems in Package will reduce component count and free up board space for additional functionality in e.g. multi-band, multi-mode communication systems. Numerous passive integration platforms are investigated and available on the market. In the laminate technology integration of capacitors with typically  $20 \text{ pF/cm}^2$ , resistors with a sheet resistance of  $35 \Omega - 1 \text{ M}\Omega$  and inductors up to  $22 \text{ nH}$  are realised [25]. Advanced technologies make use of thin film, thick film or embedded capacitors processes. In ultra-thin laminates composite capacitors with for example epoxy dielectric loaded with non-sintered barium titanate powders are developed. Capacitance densities of  $4\text{-}16 \text{ pF/mm}^2$  are reported [26]. Also polymer-silver composites are investigated to integrate capacitors with higher capacitance densities into laminates [27]. Other approaches to integrate capacitors into laminate make use of thick film or thin film technologies. In the thick film technology, capacitors are processed on Cu foil with a dielectric thickness of  $20\text{-}24 \mu\text{m}$  and a relative permittivity of 3000. The capacitors comprise a  $5 \mu\text{m}$  and  $30 \mu\text{m}$  Cu top and bottom electrode and can be integrated into the laminate. The thin film approach comprises  $300 \text{ nm}$  thick hydrothermally grown  $\text{BaTiO}_3$  on top of a titanium coated copper clad laminate. With relative permittivities of 300, capacitors with densities of  $8 \text{ nF/mm}^2$  can be integrated with these devices into laminate [28]. In an extension of these technologies also thin  $\text{BaTiO}_3$  films are deposited by sol-gel or sputter technologies on top of Cu foil. The dielectric and the top electrode are patterned and the thin film devices are integrated into laminate offering capacitance densities of  $7\text{-}50 \text{ nF/mm}^2$  [29,30,31]. The laminate technology is a relatively low-cost technology; compatible with highly conductive copper interconnects. The technology is, however, limited with respect to line width. Another passive embedded technology is the LTCC (low temperature cofired ceramic). The low dielectric loss, and the high relative permittivities that can be achieved enable the integration of a number of passive functions including capacitors, inductors, matching circuits, filters, and baluns in the substrate. Capacitors of typically  $1.5\text{-}200 \text{ pF/mm}^2$  can be integrated together with co-fired resistors of  $10\text{-}10\text{k}\Omega$  and spiral inductors of  $1\text{-}20 \text{ nH}$  [25]. The printing process in this technology limits the tolerance of the resistors.

One step further is the silicon based system in package technology, where high-value capacitors, high-quality inductors, vias and interconnect technologies are realised in high-ohmic Si substrates. This technology enables high performance decoupling capacitors, tight tolerance MIM capacitors for impedance matching as well as crude and fine via signal ground connections with highly conductive copper metallization. In the examples given in Figs. 9 and 10 (high-power front-ends and low-power transceivers for mobile communications) the high-value capacitors with capacitance densities of  $20\text{-}110 \text{ nF/mm}^2$  were achieved by trench technology, making use of low dielectric constant oxides and nitrides. These MOS capacitors are integrated with low-value MIM capacitors and high-quality inductors in a high-ohmic Si substrate. Crude vias as well as fine vias for signal/ground interconnection are developed by wet- and dry etching and subsequent metal and insulation filling [32,33]. These technologies are not limited to  $1\text{-}5 \text{ GHz}$ , but

also have enabled high performance passive functions for mm-wave applications.

With an optimum partitioning of active and passive functions into high-ohmic Si-substrates and laminate substrates, maximum performance, smallest form factor and lowest cost are achieved (see Figs 9 and 10).

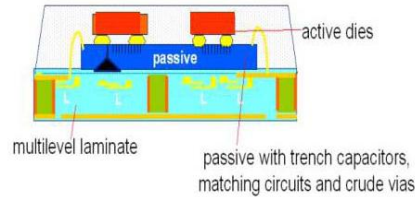


Figure 9: High-power silicon-based System in Package front-end module.

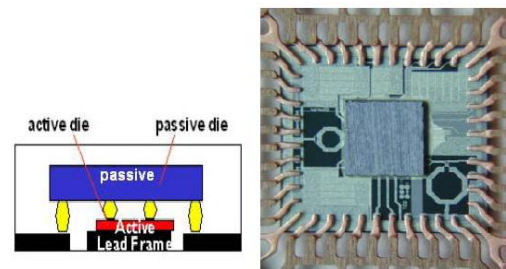


Figure 10: Low-power silicon-based System in Package transceiver.

The next step in the passive integration platform is the integration of passive and active functions in one module. Integration of high-density MIM capacitors with high-quality resistors in semiconductor compatible processes on top of Si substrates with integrated ESD protection diodes in one small chip-scale devices as realized in Fig. 11, enables a board space saving of up to 80 %.

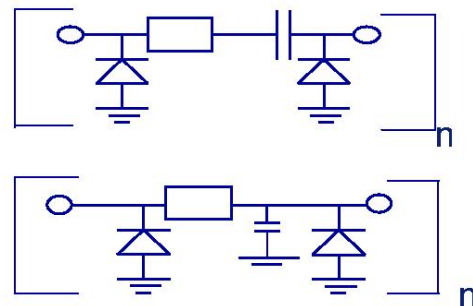


Figure 11a: High-density MIM capacitors designed to ground and in/out integrated with resistors and ESD protection diodes.

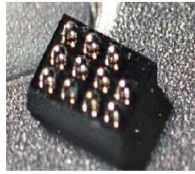


Figure 11b: High-density MIM capacitors designed to ground and in/out integrated with resistors and ESD protection diodes in small chip-scale package.

The technology developed within Philips makes use of complex oxidic thin film materials. MIM capacitors with capacitance densities of 20-110 nF/mm<sup>2</sup> and breakdown voltages of 50-180 V have been integrated with resistors of 50 Ω up to several hundred kΩ on top of Si substrates. In the Si substrate ESD protection diodes of 8, 12 and 16 kV are integrated to protect downstream components from electrostatic discharge. Due to the high breakdown voltages of the MIM capacitors this is the optimum technology to combine e.g. low-pass filtering and ESD protection for mobile communication applications.

Figure 12 shows the typical performance of two integrated low-pass filters. Both filters show an excellent matching. The performance is in very good agreement with the simulated data. In Fig. 13 the forward and reverse bias performance of the integrated ESD protection diodes is demonstrated.

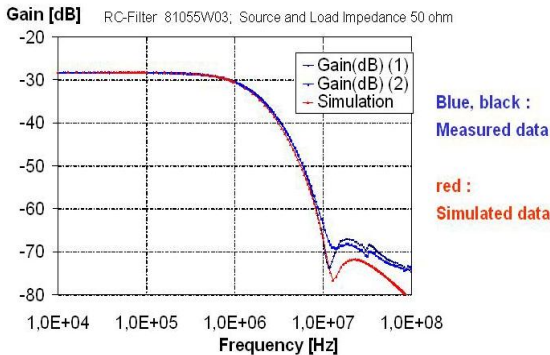


Figure 12: Two RC low-pass filters with high density MIM capacitors integrated in Si substrate next to ESD protection diodes .

This thin film passive integration platform is an innovative technology and was applied to integrate resistors with several hundred kΩ with capacitors of more than 140 nF and more than thirty ESD protection diodes in a module as small as 3.6 mm × 3.2 mm (see Fig. 14).

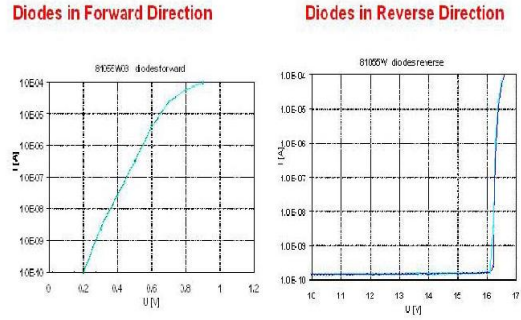


Figure 13: Current versus voltage for integrated diodes operated in forward in reverse direction.

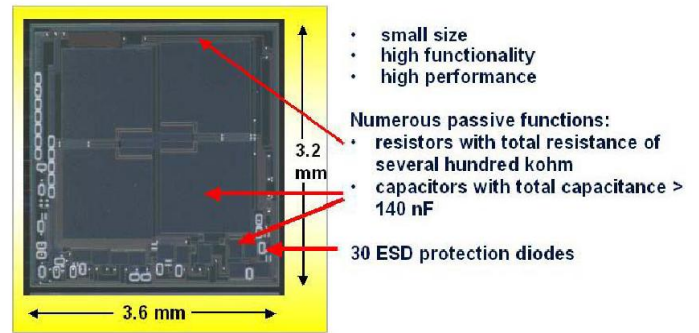


Figure 14: High density MIM capacitors with in total >140 nF integrated with resistors with in total several hundred kΩ and 30 ESD protection diodes integrated in a module of 3.6 mm × 3.2 mm.

### 3. PIEZOELECTRIC THIN FILMS FOR ULTRASONIC TRANSDUCERS

Dielectric, piezoelectric and ferroelectric thin films do not only play a role in the various passive integration platforms. They gain more and more importance also for innovative ultrasound transducers. Ultrasound systems are one of the basic imaging modalities covering cardiology, radiology, obstetrics, gynecology and general abdominal imaging. In these ultrasound systems the ultrasound transducer is the key signal generating and receiving element. Ultrasound generation and detection is performed, using piezoelectric ceramic elements. In these systems the ultrasound waves are generated by applying a voltage pulse in the poling direction of the piezoelectric ceramic, which results in a strain in the field direction (see Fig. 15).

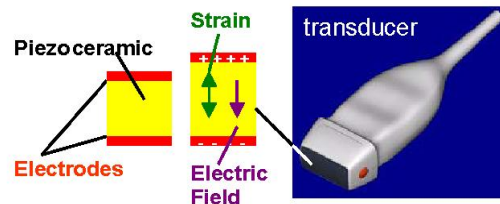


Figure 15: Thickness mode vibration of piezoelectric element.

New concepts are investigated, which make use of piezoelectric thin films, deposited on top of thin membranes. In these piezoelectric micro-machined ultrasonic transducers (PMUTs) the ultrasonic waves are generated by flexural motion of the membrane, which is coupled to strain in the piezoelectric film (see Fig. 16).

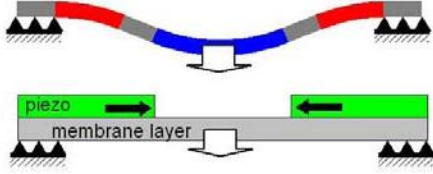


Figure 16: Piezoelectric micro-machined ultrasonic transducer principle.

Two different concepts are studied world wide on piezoelectric thin film ultrasonic transducers. For the d33 concept interdigital electrodes on top of the piezoelectric thin film, processed on the membranes are used to operate the transducer. In d31 electrodes are applied on opposite sites of the piezoelectric thin films to operate the transducer (see Fig. 17). A voltage pulse between the electrodes will result in a flexural motion and emit an acoustic wave while an incoming acoustic wave generates a voltage on the electrodes. Both the d33 [34] and the d31 concept have been studied by several groups [35].

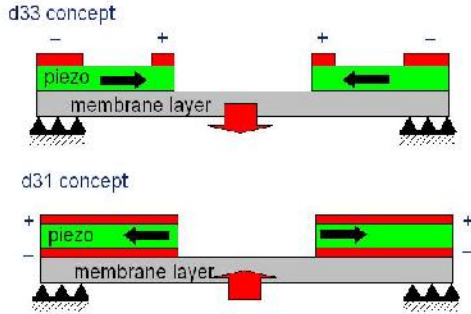


Figure 17: Piezoelectric micro-machined ultrasonic transducer concepts.

The piezoelectric properties of the thin PZT films applied in this research have been investigated in a bulk acoustic wave (BAW) resonator geometry. The advantage of this resonator geometry is that analytical simulations can be performed which provide insight into the material properties independent of the actual resonator geometry. In a BAW resonator the material coupling coefficient  $k_t$  is described via the material parameters as [38,39]

$$k_t = \frac{e}{\sqrt{c^D \epsilon^S}} \quad (1)$$

Here we have investigated two types of  $\text{PbZr}_x\text{Ti}_{1-x}\text{O}_3$  thin films with the composition at the morphotropic phase boundary. One type is (001) textured and the other type is (111) textured grown. These PZT films are sandwiched by two Pt electrodes on top of a Si substrate. To extract the material properties from the measurements, the main BAW

resonance at around 1GHz is fitted by a general one-dimensional simulation [39] which takes into account the influence of the Si substrate and both Pt electrodes. Here the Q-factors, the material coupling coefficient  $k_t$ , and the speed of sound in the PZT film are used as fit parameter while for all other parameters literature or independently measured values are used. In Fig. 18 the measured and simulated real and imaginary part of the impedance of the (001) textured PZT film is shown.

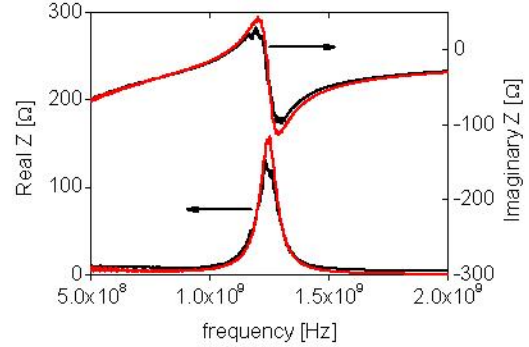


Fig. 18: Real and imaginary part of the impedance of a poled (001) oriented  $\text{PbZr}_x\text{Ti}_{1-x}\text{O}_3$  film. Measured and simulated impedance curves are shown in black and in red, respectively.

The simulated curve (red curve) follows well the measured impedance (black curve). Even small features like the small superimposed peaks due to multiple reflections at the other side of the Si substrate are correctly simulated. Also higher harmonic resonances are well reproduced (not shown). Because of the missing acoustic reflector on the Si substrate, a large amount of the energy is leaking into the Si substrate resulting in a low Q-factor of  $Q = 6$ . From the simulation the material coupling coefficients for the (001) and (111) textured PZT films are obtained in the unpoled and poled state. These values are shown in Fig. 19 in dependence of the applied electric bias field.

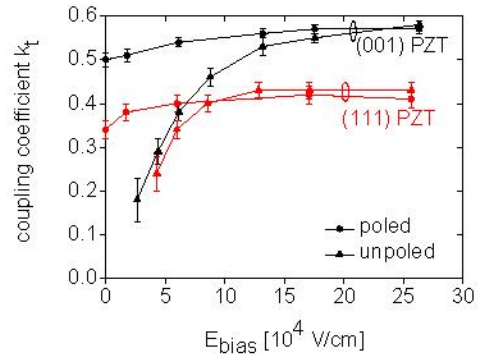


Fig. 19: Material coupling coefficient  $k_t$  of  $\text{PbZr}_x\text{Ti}_{1-x}\text{O}_3$  films with composition at the morphotropic phase boundary as a function of electric bias field. (001) and (111) oriented PZT films are shown in black and in red, respectively. Poled layers are depicted by circles and unpoled ones by triangles.

Clearly the (001) textured PZT film exhibits a higher material coupling coefficient  $k_t = 0.57$  than the (111) textured PZT film with  $k_t$  of 0.43. Furthermore, by poling of the piezoelectric layer the maximum value of  $k_t$  does not increase. Only the value at zero bias is drastically increased and the bias field is decreased at which the coupling coefficient exceeds the saturation. A comparison with the material coupling coefficient of bulk PZT (Motorola PZT 3203 HD) with  $k_t = 0.54$  [40] demonstrates the high quality of our (001) PZT thin films. The measured permittivities of the PZT films at 1kHz and 0.1V are 1110 for the (001) textured film and 990 for the more (111) textured film before poling.

The thin film ultrasonic transducers, realized here show a large bandwidth due to the excellent acoustic matching of the device to water. Measurements carried out in a water tank (see Fig. 20) for the thin film ultrasonic transducers revealed output pressures which are comparable to the best data reported so far for micro-machined ultrasonic transducers. The pressure contours measured for the thin film transducers are in excellent agreement with simulated data (see Fig. 21).

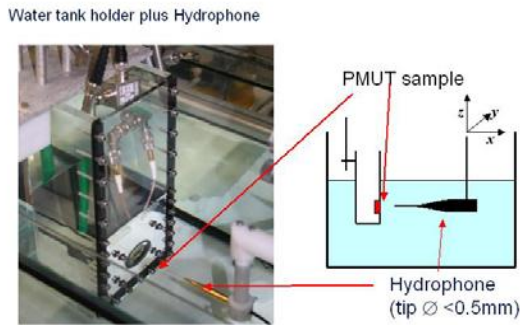


Figure 21: Piezoelectric micro-machined ultrasonic transducer tested in a water tank.

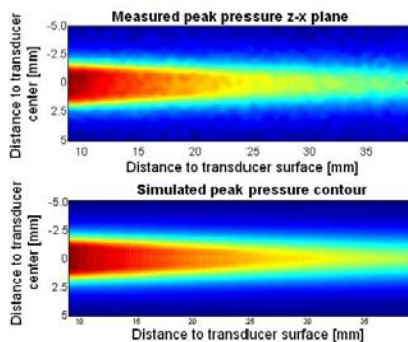


Figure 22: Measured and simulated pressure contours for piezoelectric micro-machined ultrasonic transducers.

With a number of thin film piezoelectric ultrasonic transducers, quality and reliability tests have been carried out. Test conditions have been applied as they are specified for conventional ultrasonic transducers. More than 22 billion pulses have been applied for numerous devices without any

damage. All quality and reliability tests have been passed without damage or significant performance degradation.

#### 4. CONCLUSION

Dielectric, ferroelectric and piezoelectric thin films play an important role for next generation thin film devices for mobile communication and wireless data transfer systems. The thin films open new passive integration platforms in the System in Package Technology. Capacitors with high capacitance densities and inductors can be integrated on high-ohmic Si substrates and enable a high performance silicon-based System in Package platform for RF front-end modules. Integration of high performance passive functions such as high-value MIM capacitors with resistors on low-ohmic silicon substrates offers the integration with active functions such as ESD protection diodes in small modules. These devices, which enable a size reduction of up to 80%, form a new platform of low-pass filters and protection diodes as required in the base-band, audio and power section of mobile communication systems.

Making use of the piezoelectric properties of thin films, the passive integration platform can be extended to high performance bulk acoustic wave filters and piezoelectric switches, which are requested in next generation reconfigurable RF circuits. The non-linear properties of complex oxides such as  $\text{Ba}_{1-x}\text{Sr}_x\text{TiO}_3$  thin films are an attractive route to realise integrated tunable capacitors and tunable RF filters.

Thin film piezoelectric technologies related to semiconductor processing do not only enable high performance RF filters but also open the way to piezoelectric thin film ultrasonic transducers with high quality and reliability.

#### 5. ACKNOWLEDGEMENTS

We gratefully acknowledge the co-operation with W. Brand, J. Meyer, A. Lewalter, Ch. Martiny, H. Pelzer M. Matters, J. Mills (Philips Research), C. v. Veen, J. v. Delft (Philips Apptech), M. Mienkina (U Bochum), and R.P. v. Hahn (Fachhochschule Koblenz/Remagen). Thanks are due to the European Commission for the funding of the part on tunable capacitors of this research in the EU FP6-project Nanostar.

#### 6. REFERENCES

- [1] K. M. Lakin, Proc. Ultrasonics symposium 1999, Vol. 2, 895–906
- [2] R. C. Ruby, P. Bradley, Y. Oshmyansky, A. Chien, Proc. IEEE Ultrasonics symposium 2001, Vol. 1, 813–821
- [3] K. M. Lakin, J. Belsik, J. F. McDonald, K. T. McCarron, Proc. IEEE Ultrasonics symposium 2001, Vol. 1, 833–838
- [4] M. A. Dubois, P. Muralt, V. Plesky, Proc. IEEE Ultrasonics symposium 1999, Vol. 2, 907–910

- [5] J. Kaitila, M. Yililammi, J. Molaris, J. Ellä, T. Makkonen, Proc. IEEE Ultrasonics symposium 2001, Vol. **1**, 803–806
- [6] R. Aigner, J. Kaitila, J. Ellä, L. Elbrecht, W. Nessler, M. Handtmann, T.-R. Herzog, S. Marksteiner, Proc. IEEE MTT-S Microwave Symposium 2003, Vol. **3**, 2001–2004.
- [7] H.-P. Löbl, C. Metzmacher, R.F. Milsom, A. Tuinhout, P. Lok, F. van Straten, Mater. Res. Soc. Symp. Proc. Vol. **783** ('Materials, Integration and Packaging Issues for High-Frequency Devices') (2003), 121–132.
- [8] J.D. Larson III, S. R. Gilbert, X. Baomin, Proc. IEEE Ultrasonics symposium 2004, Vol. **1**, 173–177
- [9] P. Muralt, J. Antifakos, M. Cantoni, R. Lanz, F. Martin, Proc. IEEE Ultrasonics symposium 2005, vol. **1**, 315–320
- [10] R. F. Milsom, H. P. Löbl, D. N. Peligrad, J.-W. Lobeek, A. Tuinhout, H.J. ten Dolle, Proc. IEEE Ultrasonics Symposium 2002, vol. **1**, 989–994
- [11] R. F. Milsom, H.-P. Löbl, C. Metzmacher, Proc. 2nd International Symposium on Acoustic Wave Devices for Future Mobile Communication Systems, Chiba University, Japan, p. 143, March 2004.
- [12] A.J.M. de Graauw, P.G. Steeneken, C. Chanlo, J. Dijkhuis, S. Pramm, A. van Bezooijen, H.K.J. ten Dolle, F. van Straten, P. Lok "MEMS-based reconfigurable multi-band BiCMOS amplifier", to be published at BCTM2006.
- [13] P.G. Steeneken, Th.G.S.M. Rijks, J.T.M. van Beek, M.J.E. Ulenaers, J. De Coster, R. Puers, J. Micromech. Microeng., Vol. 15, pp. 176-184 (2005)
- [14] J.T.M. van Beek, P.G. Steeneken, G.J.A.M. Verheijden, J.W. Weekamp, A. den Dekker, M. Giesen, A.J.M. de Graauw, J.J. Koning, F. Theunis, P. van der Wel, B. van Velzen, P. Wessels, Proceedings MEMSwave2006, session 5, paper 17.
- [15] S.J. Gross, Q.Q. Zhang, S. Trolier-McKinstry, S. Tadigadapa, T.N. Jackson, Device Research Conference, 2003, 99–100
- [16] A. Vorobiev, P. Rundqvist, K. Khamchane, and S. Gevorgian, J. Appl. Phys., Vol. 96, 4642–4649 (2004)
- [17] T. S. Kalkur, Ch. Cotey, K. Chen, Sh. Sun, Integrated Ferroelectrics, 56, 1123–1159 (2003)
- [18] J.-P. Maria, C.B. Parker, A.I. Kingon, G. Stauf, Proc. IEEE ISAF2002, 151–154 (2002)
- [19] A. K. Tagantsev, V. O. Sherman, K. F. Astafiev, J. Venkatesh, and N. Setter, J. Electroceramics, Vol. **11**, 5–66, (2003)
- [20] Y. Yoon et al., IEEE Trans. MTT, Vol. **51**, 2568 (2003)
- [21] S. V. Razumov, A. V. Tumarkin, M. M. Gaidukov, A. G. Gagarin, A. B. Kozyrev, O. G. Vendik, A. V. Ivanov, O. U. Buslov, V. N. Keys, L. C. Sengupta, and X. Zhang, Appl. Phys. Lett., Vol. **81**, 1675–1677 (2002)
- [22] A. Eriksson, A. Deleniv, and S. Gevorgian, IEEE Trans. Appl. Supercond., Vol. **14**, (2004)
- [23] R. York, A. Nagra, E. Erker, T. Taylor, P. Periaswamy, J. Speck, S. Streiffer, O. Auciello, Proc. IEEE Int. Sym. Appl. Ferroelectrics ISAF2000, Vol. **1**, 195–200 (2000)
- [24] See, e.g., <http://www.agilematerials.com>, <http://www.paratek.com>, <http://www.ngimat.com>, <http://www.gennum.com>
- [25] J. Wu, M. Anderson, D. Collier, G. Guth, Proc. ICEPT, 484–490 (2003)
- [26] J. Pfeifer, Printed Circuit Design and Manufacture, 40–42 April 2004
- [27] Y. Rao, C. Wong, 2002 Electronic Components and Technology Conference, 920–923 (2002).
- [28] D. Balaraman, J. Electroceramics, Vol. **13**, 95-100 (2004).
- [29] T. Kim, S. Srinivasan, and A.I. Kingon, Mater. Res. Soc. Symp. Proc. Vol. **902E**, 0902-T02-05.1–6;
- [30] B. Laughlin, J. Ihlefeld, and J.P. Maria, J. Am. Ceram. Soc. **88**, 2652-2654 (1005)
- [31] J. Ihlefeld, A. I. Kingon, W. Borland and J.-P. Maria, Mat. Res. Soc. Symp. Proc. Vol. 783, B.3.2.1. – B.3.2.6. (2004)
- [32] F. Roozeboom, A. Kemmeren, J. Verhoeven, F. van den Heuvel, H. Kretschman and T. Frič, , Mat. Res. Soc. Symp. Proc. Vol. **783**, 157–162 (2003)
- [33] F. Roozeboom, A.L.A.M. Kemmeren, J.F.C. Verhoeven, F.C. van den Heuvel, J. Klootwijk, H. Kretschman, T. Frič, E.C.E. van Grunsven, S. Bardy, C. Bunel, D. Chevrie, F. LeCorneec, S. Ledain, F. Murray and P. Philippe, Thin Solid Films, Vol. **504**, 391–396 (2006)
- [34] Bernstein, IEEE Ultrasonics Symposium 1999, Vol. **1**, 1145 (1999)
- [35] P. Muralt et al., IEEE Trans. UFFC, Vol. **52**, 2276 (2005)
- [36] M. Schreiter et al., J. Eur. Cer. Soc., Vol. **24**, 1589–1592 (2004)
- [37] S. Gevorgian, A. Vorobiev, and T. Lewin, J. Appl. Phys., Vol. **99**, 124112 (2006)
- [38] IEEE Standard on Piezoelectricity, No. 176 (1987).
- [39] H. Nowotny and E. Benes, J. Acoust. Soc. Am., Vol. 82, 513 (1987).
- [40] R. L. Thayer, C. A. Randall, and S. Trolier-McKinstry, J. Appl. Phys., Vol. **94**, 1941–1947 (2003)
- [41] Jiwei Lu Appl. Phys. Lett., Vol. **88**, 112905 (2006)